Proceedings of IDETC/CIE 2009
ASME 2009 International Design Engineering Technical Conferences &
Computers and Information in Engineering Conference
August 30 - September 2, 2009, San Diego, California, USA

DETC2009-87083

LEVEL SET BASED ROBUST SHAPE AND TOPOLOGY OPTIMIZATION UNDER RANDOM FIELD UNCERTAINTIES

Shikui CHEN
Dept. of Mechanical Engineering
Northwestern University,
2145 Sheridan Road, Tech. B224,
Evanston, IL, 60208.
shikui-chen@northwestern.edu

Sanghoon LEE
Korea Atomic Energy Research Institute
Deokjin-dong 150-1, Yuseong-gu,
Daejeon, 305-353
Republic of Korea
shlee1222@kaeri.re.kr

Wei CHEN*
Dept. of Mechanical Engineering
Northwestern University,
2145 Sheridan Road, Tech. B224,
Evanston, IL, 60208.
weichen@northwestern.edu

ABSTRACT

A level-set-based method for robust shape and topology optimization (RSTO) is proposed in this work with consideration of uncertainties that can be represented by random variables or random fields. Uncertainty, such as those associated with loading and material, is introduced into shape and topology optimization as a new dimension in addition to space and time, and the optimal geometry is sought in this extended space. The level-set-based RSTO problem is mathematically formulated by expressing the statistical moments of a response as functionals of geometric shapes and loading/material uncertainties. Spectral methods are employed for reducing the dimensionality in uncertainty representation and the Gauss-type quadrature formulae is used for uncertainty propagation. The latter strategy also helps transform the RSTO problem into a weighted summation of a series of deterministic topology optimization subproblems. The above-mentioned techniques are seamlessly integrated with level set methods for solving RSTO problems. The method proposed in this paper is generic, which is not limited to problems with random variable uncertainties, as usually reported in other existing work, but is applicable to general RSTO problems considering uncertainties with field variabilities. This characteristic uniquely distinguishes the proposed method from other existing approaches. Preliminary 2D and 3D results show that RSTO can lead to designs with different shapes and topologies and superior robustness compared to their deterministic counterparts.

NOMENCLATURE

$C(x_1, x_2)$	spatial covariance function
$\mathbf{D}$	spatial domain
E_{ijkl}	elastic tensor
$g(x,\omega)$	random field
$\bar{g}(x)$	mean function of $g(x,\omega)$
$g_i(x)$ or $\mathbf{g}_i$	the ith eigenfunction
J	objective functional
$p(z)$	joint probability density function
u	state variable
$\mathbf{V}(x)$	design velocity field
w_i	weight of the ith quadrature point
ϕ	level set function
λ	Lagrange multiplier
λ_i	the ith eigenvalue
$\xi_i(\omega)$	orthogonal random variables with zero mean and unit variance
μ	mean performance
σ^2	performance variance
z	random quantities
Θ	sample space
ω	an element of the sample space Θ
Ω	geometric shape of the design
$\partial\Omega$	boundary of Ω

1. INTRODUCTION

Since the seminal work of Bendsøe and Kikuchi [1], structural topology optimization has undergone considerable developments during the past two decades, which provides an efficient way to obtain effective design candidates and greatly accelerates the engineering design innovation process. The underlying idea of topology optimization is to recast a design problem as an optimal material distribution problem, where an optimal configuration of the design is sought to optimize the design requirements measured quantitatively by an objective function. The state-of-the-art topology optimization approaches include the ground structure method [2], the homogenization method [1], the power-law approach [3] which is also called simple isotropic material with penalization (SIMP) [4, 5], and the level set methods [6-9]. Although topology optimization is

* Corresponding Author: Dr. Wei Chen, Professor of Mechanical Engineering, Northwestern University, 2145 Sheridan Road, Tech. B224, Evanston, IL, USA, 60208.

becoming a matured field, most of the current work is focused on deterministic optimization where the design is achieved without consideration of various sources of uncertainties, such as the variation in the loading, material properties, or geometric variations due to the imprecise manufacturing process. To obtain robust and reliable designs, the uncertainties existing in the structure and its operating environment need to be considered and their impact on design performance should be assessed quantitatively during a design process. Topology optimization under uncertainties is still an open research area which requires further investigations. The difficulties are attributed to the infinite-dimensional property of topology optimization, which poses great challenges in uncertainty quantification, propagation, and design sensitivity analysis.

Recent years have seen growing interests in taking uncertainty into account to obtain robust and reliable topological designs. Due to its simplicity, frame structures were first studied for robust and reliability-based topology optimization under uncertainty, respectively [10-12]. Olhoff et al. first integrated reliability analysis into the element-based topology optimization method and introduced a new strategy called reliability-based topology optimization (RBTO) [13], where a probabilistic constraint is introduced, while the objective is treated as deterministic. Reliability-based topology optimization was further developed in recent years by different research groups [14-19]. A comprehensive review of RBTO can be found in [20]. On the other hand, not many works, except [12, 21, 22], exist on robust topology optimization (RTO), although it is a topic of great significance both in academic and industrial applications.

Robust optimization problems have been addressed in different scientific disciplines [23]. The first approach is the method of stochastic programming [24] with its root in operations research; the second method is robust design [25], originating in engineering design. Among the existing RTO works, Seepersad et al. employed the frame structure method and the robust design approach to implement robust topology optimization of cell structures considering uncertain boundary conditions [12]. The limitation in the frame-structure based RTO method lies in the fact that the configuration of the optimal design is determined to a large extent by the number and locations of the nodes of the frame structure. If the number of nodes is limited, the solution may not be sufficient to represent the optimal topology. Using the homogenization method, Kogiso et al. [21] proposed a sensitivity-based RTO method for designing compliant mechanisms, where the effect of the variations in the direction of the input force on the output displacement is considered. The variations of the output displacement are evaluated using the first-order derivative. Conti's work [22] is the first to combine level set methods with stochastic programming techniques for structural optimization under loading uncertainties. Different from Conti's work, we solve RSTO problems by integrating the level set methods with the robust design formulation considering not only the random variable uncertainty, but also random field uncertainties. Conventional robust design optimization is usually set as a continuous optimization problem in finite dimensions. To combine robust design with shape and topology optimization, which is an infinite-dimensional optimization problem, we define the statistical moments of the response as functionals of geometric shapes and a set of random parameters reduced from random field. With the newly-introduced dimension of uncertainty, the optimal geometric shape is sought to simultaneously optimize the expectation of the design performance and minimize its variance. A basic issue to be addressed in RSTO is how to characterize the uncertainties and propagate them to the design responses in an efficient manner. In this paper, the spectral method [26], in particular, the Karhunen-Loeve expansion is employed to reduce the dimensionality in uncertainty representation. After that, the statistical moments of design responses are evaluated using the generalized Gauss-type quadrature, and the shape sensitivity of the statistics is derived using the adjoint variable method. The shape derivative is further combined with a steepest descent method to form a design velocity filed for the level set equation to update the design solution in optimization iterations. The level set methods offer a precise boundary description for implementing both the robust shape optimization and topology optimization in a unified mathematical framework, which is another advantage of the proposed method.

This paper is organized as follows: A brief review of robust optimization and fundamentals about level set methods for RSTO are presented in Section 2. After that, uncertainty characterization and propagation using the spectral method and the Gauss-type quadrature will be introduced in Section 3. In Section 4, the shape derivatives of the statistical moments are derived using the adjoint variable method. The numerical algorithm for RSTO together with three demonstration examples are provided in Section 5. Conclusions and future works are discussed in the last section.

2. LEVEL-SET BASED ROBUST SHAPE AND TOPOLOGY OPTIMIZATION (RSTO)

2.1 Robust design models

Conventional robust design, pioneered by Taguchi [27], refers to a class of methods for improving quality and reliability by designing a product or process so that it is robust (insensitive) against variations in uncontrollable noise variables [28-30]. The robust design problem typically involves a nonlinear programming formulation [25, 31-33] in which the objective is to make suitable tradeoff between 'optimizing' the mean performance μ and minimizing the performance variance σ^2 (or the standard deviation σ), as shown in Figure 1.

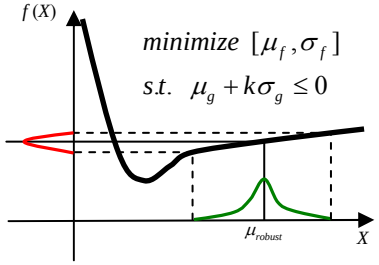

FIGURE 1: ROBUST DESIGN MODEL [25].

The actual objective function to be minimized represents a designer's preference in this tradeoff [34]. The common robust design objective function balances between the mean and variance of the objective response through the choice of the

constant c [35-40]. Functions of the form $\mu + c\sigma$ also play a role when we have constraint responses that must satisfy certain conditions with specified probabilities. When the constraints relate to the failure of a product, the constraint evaluation is often referred to as reliability assessment [41-44]. For a more complete review on robust optimization, please be referred to literatures [20, 23, 25].

2.2 Level Set Methods for Shape and Topology Optimization

Level set methods were originally introduced by Osher and Sethian [45] as a numerical scheme for tracking fronts propagating with curvature-dependent speed. In the past two decades, level set methods have thrived to be powerful tools with many applications in different fields [46, 47]. Their advantage lies in their capability of precisely describing closed boundaries with dynamic variations, which enables easy 'capture' of the boundary on an Euler grid by solving a Hamilton-Jacobi partial differential equation [48]. Sethian and Wiengmann [49] first combined level set methods with the immersed interface methods for structural boundary design, where the former was used to represent the geometric boundary of the design and the latter was used for elastic analysis. Osher and Santosa [50] introduced the shape gradient of the objective functional into the level set model and established a link between the shape gradient and the velocity field. This work was further completed by Allaire et al. [7, 51], who derived the shape sensitivity of compliance and geometric advantage by employing the adjoint variable method. Starting from the material derivative method [9, 48], Wang et al. [48] identified a meaningful link between the velocity field in the level set method and the general structural sensitivity analysis. The 'color level set' model, which was also proposed by Wang [9], made possible the topology optimization of multi-material structures and compliant mechanisms in the level set framework [52-55]. To avoid being lost in technical details, in this section, we only focus on the key issues involved in RSTO. A complete introduction to level set methods can be found in [46, 47].

As its name implies, level set method implicitly represents the boundary as the zero level set of a one-higher dimensional surface $\phi(x)$, which is called the level set function. In the level set model, the domain is defined as three parts according to the value of the level set function:

$$\begin{cases} \phi\big(x(t)\big) > 0 & : \quad x(t) \in D \setminus \Omega \\ \phi\big(x(t)\big) = 0 & : \quad x(t) \in \partial\Omega \\ \phi\big(x(t)\big) < 0 & : \quad x(t) \in \Omega \setminus \partial\Omega \end{cases}, \tag{1}$$

where D denotes the design domain; and $t \in R^+$ is time. The domain and a sketch of level set representation are shown in Figure 2. The greatest advantage of implicit representation lies in its ability of dealing with topological changes, such as splitting and merging of the boundary, in a natural manner.

By calculating the material derivative [56] of the equation $\phi\big(x\big) = 0$, we get the following equation:

$$\frac{\partial \phi}{\partial t} + \nabla\phi \cdot \mathbf{V}(x) = 0, \tag{2}$$

where $\mathbf{V}(x) = \dfrac{dx}{dt}$ is the velocity vector field. Considering $\mathbf{n} = \dfrac{\nabla\phi}{|\nabla\phi|}$ and $\mathbf{V}\cdot\nabla\phi = \big(\mathbf{V}\cdot\mathbf{n}\big)|\nabla\phi|$, we can write equation (2) as

$$\frac{\partial \phi}{\partial t} + V_n(x)|\nabla\phi| = 0. \tag{3}$$

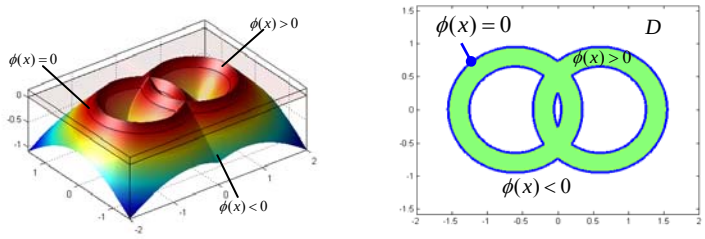

(a) 3D level set function **(b) corresponding 2D geometry**

FIGURE 2: A 2D BOUNDARY EMBEDDED AS THE ZERO LEVEL SET OF A 3D LEVEL SET FUNCTION

These two Hamilton-Jacobi type partial differential equations (PDEs) are the well-known level set equations [45-47]. Based on the level set theory, the topology optimization problem is transformed into a problem of finding the steady-state solution of the Hamilton-Jacobi equation. To get a feasible steady-state solution of equations (2) and (3), an important issue is to find the velocity field. More details on calculating the shape derivative and identifying the velocity field in the RSTO problem will be provided in Section 5.

2.3 Setting an RSTO Problem

In probabilistic RSTO, uncertainty is introduced as a new dimension in addition to space and time [57], while the solution is sought in this extended space. Let's use z to denote the random quantities, and assume z is independent of the design variable shape Ω. The design response (performance) under uncertainties can be correspondingly expressed as a functional $J(\Omega, u, z)$ of the random quantities z in addition to the geometric shape Ω and state variable u, that is

$$J(\Omega, u, z) = \int_\Omega f\big(u(\Omega, z)\big) d\Omega, \tag{4}$$

where the performance function $J(\Omega, u, z)$ is the total strain energy, or the mean compliance, of the structure in structural optimization; in complaint mechanism optimization, $J(\Omega, u, z)$ is the geometric advantage/work efficiency. The random quantity considered here can have field variability to form a random field or random process but it can always be descretized into a finite number of random parameters, which will be further explained in Section 3.1. Thus equation (4) is general enough to cover random field or random process.

The mean $\mu(J(\Omega, u, z))$ and standard derivation $\sigma(J(\Omega, u, z)$ of the response $J(\Omega, u, z)$ in equation (4) can be further expressed as follows

$$\mu(J(\Omega, u, z)) = \iint_\Omega p(z) f\big(u\big(\Omega, z\big)\big) d\Omega dz = \int p(z) J(\Omega, u, z) dz,$$

$$Var(J(\Omega,u,z))$$
$$= \int p(z)\left[\int_\Omega p(z) f\left(u(\Omega,z)\right)d\Omega - \iint_\Omega p(z) f\left(u(\Omega,z)\right)d\Omega dz\right]^2 dz$$
$$= \int p(z)\left[J(\Omega,u,z) - \mu\left(J(\Omega,u,z)\right)\right]^2 dz, \tag{5}$$

where $p(z)$ is the joint probability density function (p.d.f.) of the random variables. In this way, an RSTO problem is set as follows:

Minimize

$$J^*(\Omega,u,z) = \mu(J(\Omega,u,z)) + c\sigma(J(\Omega,u,z)$$

Subject to: (6)

$$\textit{Volume constraint}\,|\Omega| = |\Omega|_{obj},$$

$$\textit{Perimeter constraint on}\,|\partial\Omega|,$$

together with the partial differential equations (PDEs) governing the physical system.

3. UNCERTAINTY QUANTIFICATION AND PROPAGATION IN RSTO

Using the probability theory, uncertainties in structural optimization can be modeled either as random variables or random fields [58]. For example, when considering a concentrated random load, as shown in Figure 3(a), we can model its magnitude and direction as two random variables, either correlated or independent. However for problems with distributed loads with spatial variability in directions or magnitudes as shown in Figure 3(b) or a piece of material with properties varying across the spatial domain as shown in Figure 8(b), the loadings and material properties should be more realistically modeled as random fields [58, 59]. Our research goal in this work is to develop a mathematically rigorous and computationally viable approach to RSTO problems under such uncertainties.

To propagate uncertainty in a RSTO process, we propose to use the Gauss-type quadrature formula which is applicable to arbitrary probability distributions. The uncertainty modeled by a random field needs to be discretized into a finite number of random variables for practical manipulations. In this section, we first discuss the discretization of random fields using spectral representation and the propagation of uncertainty based on the Gauss-type quadrature formula. These methods are further incorporated into the framework of level-set based robust topology optimization.

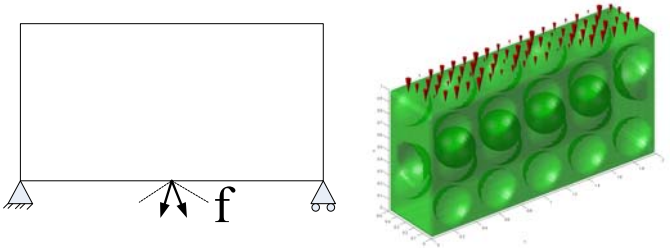

(a) a lumped random load **(b) a random loading field**

FIGURE 3: SKETCHES OF A LUMPED RANDOM LOAD AND A RANDOM LOADING FIELD

3.1 Karhunen-Loeve Expansion of Random Field

The Karhunen-Loeve expansion [60] is a spectral approach to represent a random field using eigenfunctions of the random field's covariance function as expansion bases. Let $g(x,\omega)$ $: D\times\Theta \to \mathbb{R}$ be a random field defined over a spatial domain $\mathbf{D}$, which is a function of spatial coordinate x. Here $\omega \in \Theta$ denotes an element of the sample space and is used to indicate that the involved quantity is random. $g(x,\omega)$ can be represented by the K-L expansion as follows:

$$g(x,\omega) = \bar{g}(x) + \sum_{i=1}^{\infty}\sqrt{\lambda_i}\,g_i(x)\xi_i(\omega), \tag{7}$$

where $\bar{g}(x)$ is the mean function. λ_i and $g_i(x)$ are the ith eigenvalue and eigenfunction obtained from the following integral equation:

$$\int_{\mathbf{D}} C(x_1,x_2)g_i(x_1)dx_1 = \lambda_i g_i(x_2), \tag{8}$$

where $C(x_1,x_2)$ is the spatial covariance function of the random field $g(x,\omega)$. The random field variables, $\xi_i(\omega)$ in Eqn. (7) are orthogonal random variables with zero mean and unit variance. That is,

$$E\left(\xi_i(\omega)\right) = 0 \text{ and } E\left(\xi_i(\omega)\xi_j(\omega)\right) = \delta_{ij}. \tag{9}$$

The orthogonality of $\xi_i(\omega)$ is a unique feature of the K-L expansion. $\xi_i(\omega)$ can be calculated as:

$$\xi_i(\omega) = \frac{1}{\sqrt{\lambda_i}}\int_D \left(g(x,\omega) - \bar{g}(x)\right)g_i(x)dx \tag{10}$$

The second order statistics of $\xi_i(\omega)$ in Eqn. (9) can be derived from Eqn. (10). Based on sampling and spatial integration at the right side of Eqn. (10), samples of $\xi_i(\omega)$ can be generated to infer the distribution of the random field variable, $\xi_i(\omega)$. The K-L expansion is the optimal among finite representations using orthogonormal bases in the sense that the mean square error caused by a truncation of the expansion is minimized [60].

When applying the K-L expansion to a discretized random field, operations on functions are transformed into operations on matrices [61]. A random field can be spatially discretized by the spatial averaging method or the collocation method [62]. Let $\mathbf{g}(\omega)$ denote an N dimensional random vector whose elements are random variables obtained by discretizing a random field $g(x,\omega)$ at N observation points in the domain D. The K-L expansion of $\mathbf{g}(\omega)$ can be expressed as:

$$\mathbf{g}(\omega) = \bar{\mathbf{g}} + \sum_{i=1}^{N}\sqrt{\lambda_i}\,\mathbf{g}_i\xi_i(\omega), \tag{11}$$

where $\bar{\mathbf{g}}$ denotes a vector containing the mean values of the random field g at the N observation points; λ_i and $\mathbf{g}_i$ are the eigenvalues and eigenvectors of the covariance matrix C; $\xi_i(\theta)$ are orthogonal random field variables with zero mean and unit variance. By truncating Eqn. (11) at some $M \ll N$, a reduced order K-L representation of random field can be

obtained with its significance of representing the random field measured as:

$$s = \sum_{i=1}^{M} \lambda_i \Big/ \sum_{i=1}^{N} \lambda_i \ . \tag{12}$$

When s is sufficiently close to one, a reduced order representation (Eqn. (11) with $N = M$) can be used to represent the random field with a much smaller dimensionality (M) without sacrificing too much of the accuracy. The benefits of such reduction will be further demonstrated in our example problems. The procedure illustrated above can also be used to characterize a random field from data obtained at a finite number of observation points in a spatial domain [61].

3.3 Multivariate Gauss-type Quadrature for statistical moments calculation

Multivariate quadrature formulas for multiple random variables can be built from one dimensional quadrature formulas [59]. There are many ways of doing this [63] and in this paper, we focus our examination on two methods, the tensor product quadrature (TPQ) formula and the univariate dimension reduction (UDR) method.

With the TPQ formula, the k-th statistical moments of $g(\mathbf{X})$ can be calculated as:

$$\begin{aligned} E\left[g^k\right] &= \int_{\Omega_1} \cdots \int_{\Omega_n} \left\{g\left(x_1, \cdots, x_n\right)\right\}^k f_{\mathbf{X}}(\mathbf{x})\, d\mathbf{x} \\ &\simeq \sum_{i_1=1}^{m_1} w_{1\cdot i_1} \cdots \sum_{i_n=1}^{m_n} w_{1\cdot i_n} \left\{g\left(l_{1\cdot i_1}, \cdots, l_{n\cdot i_n}\right)\right\}^k \end{aligned} \tag{13}$$

where $f_{\mathbf{X}}(\mathbf{x})$ is the joint PDF of $\mathbf{X}$ and $l_{i\cdot j}$, $w_{i\cdot j}$ are the j-th node and weight of the i-th variable. Ω_i, m_i are the domain of integration and the number of nodes for i-th variable, respectively. The total number of $g(\mathbf{x})$ evaluations is $m_1 \times m_2 \cdots \times m_n$.

The central moments can be calculated from the raw moments obtained by (13) or directly calculated as in (13) with $g(\mathbf{x})$ replaced by $g(\mathbf{x}) - \mu_g$. Expressions for the mean, standard deviation are as follows:

$$\text{(mean)} \quad \mu_g = \sum_{i_1=1}^{m_1} w_{1\cdot i_1} \cdots \sum_{i_n=1}^{m_n} w_{n\cdot i_n}\, g\left(l_{1\cdot i_1}, \cdots, l_{n\cdot i_n}\right), \tag{14}$$

$$\text{(STD)} \quad \sigma_g = \left[\sum_{i_1=1}^{m_1} w_{1\cdot i_1} \cdots \sum_{i_n=1}^{m_2} w_{n\cdot i_n} \left(g\left(l_{1\cdot i_1}, \cdots, l_{n\cdot i_n}\right) - \mu_g\right)^2\right]^{1/2},$$

With the univariate dimension reduction (UDR) method [64], the multivariate function $g(\mathbf{X})$ is approximated by a sum of univariate functions which depend on only one variable with the other variables fixed to their mean values. Let the univariate functions denoted by $g_{\_i}$, then $g(\mathbf{X})$ is approximated as follows:

$$\begin{aligned} g(\mathbf{X}) \simeq \hat{g}(\mathbf{X}) &= \sum_{i=1}^{n} g\left(\mu_1, \cdots, X_i, \cdots, \mu_n\right) - (n-1)\, g\left(\mu_1, \cdots, \mu_n\right) \\ &= \sum_{i=1}^{n} g_{\_i}\left(X_i\right) - (n-1)\, g\left(\boldsymbol{\mu}_{\mathbf{X}}\right) \end{aligned} \tag{15}$$

Here independence of X_i is assumed and it is known that the error of this approximation is mainly contributed from the interaction effects among variables [65]. Since X_i are mutually independent, $g_{\_i}(X_i)$ are also independent with each other and the statistical moments of $\hat{g}(\mathbf{X})$ can be approximated conveniently from moments of $g_{\_i}(X_i)$, as follows [66]:

$$\text{(Mean)} \quad \mu_{\hat{g}} = \sum_{i=1}^{n} \mu_{g_{\_i}} - (n-1)\, g\left(\boldsymbol{\mu}_{\mathbf{X}}\right), \tag{16}$$

$$\text{(STD)} \quad \sigma_{\hat{g}}^2 = \sum_{i=1}^{n} \sigma_{g_{\_i}}^2 \ ,$$

The moments of univariate functions are calculated using one dimensional Gauss-type quadrature formula. The number of $g(\mathbf{x})$ evaluations for this calculation is $m_1 + \cdots + m_n + 1$ where m_i is the number of nodes used for the calculation of moments of $g_{\_i}$. The UDR method offers a much efficient approach than the TPQ method, however, the method might not be accurate when there exists strong interactions between random variables [67].

4. SHAPE DERIVATIVES OF STATISTICAL MOMENTS

To minimize the objective functional formulated in equation (6), we need to quantify the change of the objective functional $J^*(\Omega, u, \omega)$ with respect to a small variation of the shape Ω (design), which can provide us with necessary information for updating the current design. This process is called shape sensitivity analysis and the result is called shape derivative [68]. In this section, a semi-analytical shape sensitivity analysis approach is presented. The mean and variance of the response are first numerically discretized using the multivariate Gauss-type quadrature discussed in Section 3.3. From an optimization point of view, the multivariate Gauss-type quadrature essentially transforms the RTO problem into a weighted summation of a series of deterministic topology optimization subproblems. The shape sensitivity of each subproblem is then derived using the adjoint variable method and calculus of variation.

Equations (6) can be approximated by using either the TPQ formula in equations (14) or the UDR formula in equations (15) and (16). For simplicity, we use the TPQ formula here as an example to illustrate how to derive the shape gradient of the statistical moments. Shape sensitivity analysis with UDR formula can be derived in a similar way.

$$\begin{aligned} \mu(J(\Omega, u, \omega)) &= \sum_{i=1}^{n} w_i J(\Omega, u, \omega_i), \\ Var(J(\Omega, u, \omega)) &= \sum_{i=1}^{n} w_i \left[J(\Omega, u, \omega_i) - \mu\right]^2, \end{aligned} \tag{17}$$

where ω_i is a realization of the random variables, w_i is the corresponding weight to each quadrature point and n is the number of quadrature points. We address the general problem using the variational method and the techniques proposed in [51, 69, 70]. With the assumption that the random variables are

independent of the design variables Ω, the shape derivatives of the mean and variance of the performance function $J(\Omega,u,\omega)$ can be expressed as follows:

$$\mu_\Omega(J(\Omega,u,\omega)) = \int p(\omega)J_\Omega(\Omega,u,\omega)d\omega. \tag{18}$$

Using the Gauss-type quadrature formula [67], equation (18) is numerically approximated by

$$\mu_\Omega(J(\Omega,u,\omega)) = \sum_{i=1}^{n} w_i J_\Omega(\Omega,u,\omega_i), \tag{19}$$

Similarly, the shape derivative of the variance can be expressed as:

$$Var_\Omega(J(\Omega,u,\omega)) \approx 2\sum_{i=1}^{n} w_i \left\{ \begin{bmatrix} J(\Omega,u,\omega_i) - \mu\left(J(\Omega,u,\omega)\right) \end{bmatrix} \atop \begin{bmatrix} J_\Omega(\Omega,u,\omega_i) - \mu_\Omega\left(J(\Omega,u,\omega)\right) \end{bmatrix} \right\} \tag{20}$$

The final shape derivative of the objective functional $J^*(\Omega,u,\omega)$ is

$$\begin{aligned} &J^*{}_\Omega(\Omega,u,\omega) = \mu_\Omega(J(\Omega,u,\omega)) + c\sigma_\Omega(J(\Omega,u,\omega)) \\ &= \sum_{i=1}^{n} w_i J_\Omega(\Omega,u,\omega_i) + \frac{c}{\sigma(J(\Omega,u,\omega))}\cdot \\ &\sum_{i=1}^{n}\left\{ w_i\left[J(\Omega,u,\omega_i) - \mu\left(J(\Omega,u,\omega)\right)\right]\left[J_\Omega(\Omega,u,\omega_i) - \mu_\Omega\left(J(\Omega,u,\omega)\right)\right]\right\} \\ &= \sum_{i=1}^{n} w_i J_\Omega(\Omega,u,\omega_i) + \frac{c}{\sigma(J(\Omega,u,\omega))}\cdot \\ &\sum_{i=1}^{n} w_i\left[J(\Omega,u,\omega_i) - \mu\left(J(\Omega,u,\omega)\right)\right]\left[J_\Omega(\Omega,u,\omega_i) - \sum_{i=1}^{n} w_i J_\Omega(\Omega,u,\omega_i)\right] \end{aligned} \tag{21}$$

In this way, the shape sensitivity of $J^*{}_\Omega(\Omega,u,\omega)$ can be transformed into a weighted summation of the shape sensitivities of a series of deterministic scenarios. $J_\Omega(\Omega,u,\omega_i)$ reveals the underlying relations between the design variable shape Ω and the objective functional $J(\Omega,u,\omega_i)$ under a specified load scenario with the random parameter ω_i. In order to calculate equation (21), which is the shape derivative of the weighted summation of the expectation and variance of the performance function, we need to calculate the shape sensitivity $J_\Omega(\Omega,u,\omega_i)$ for each scenario with the random parameter ω_i. In this work, we consider a linear elastic system and take the structure compliance as the performance function $J(\Omega,u,\omega_i)$. Since in each scenario the random parameter ω_i is a constant, we briefly write $J(\Omega,u,\omega_i)$ as $J(\Omega,u)$ in the following derivation process. The compliance of the elastic system may be formulated as follows:

$$J(\Omega,u) = \int_\Omega E_{ijkl}\varepsilon_{ij}(u)\varepsilon_{kl}(u)d\Omega, \tag{22}$$

At the same time, the system is subject to the linear equilibrium equation

$$W(u,v) = a(u,v) - l(v) = 0, \tag{23}$$

Here

$$a(u,v) = \frac{1}{2}\int_\Omega E_{ijkl}\varepsilon_{ij}(u)\varepsilon_{kl}(v)d\Omega \tag{24}$$

describes the virtual work stored in the deformed system. Note that $a(u,v)$ is a symmetric bilinear functional [56], which means $a(u,v)$ is linear both in displacement u and virtual displacement v, that is, $a(u,v) = a(v,u)$. The functional

$$l(v) = \int_\Omega fvd\Omega + \int_\Gamma gvds \tag{25}$$

describes the virtual work done by external load. $l(v)$ is a linear functional depending on loading $f(\omega_i)$ and $g(\omega_i)$, where $f(\omega_i)$ is the body force and $g(\omega_i)$ is the surface traction. Note that $f(\omega_i)$ and $g(\omega_i)$ depend on a realization of the random parameter ω_i.

$$\begin{aligned} L(u,v) &= a(u,u) + \lambda\left[a(u,v) - l(v)\right] \\ &= a(u,u) + a(u,\lambda v) - l(\lambda v) \end{aligned}. \tag{26}$$

Since v is an arbitrary displacement field in the admissible displacement space, after being multiplied by a scalar λ, λv still falls into the same linear space. We can further simplify the above equation with only v:

$$L(u,v) = a(u,u) + a(u,v) - l(v) \tag{27}$$

The weak form of the adjoint variable equation can be expressed as the derivative of functional L in the direction of ψ, which may be described in an inner product form as follows:

$$\begin{aligned} &< \frac{\partial L}{\partial u}, \psi > \equiv 0 \Rightarrow \lim_{\tau\to 0}\frac{L(u+\tau\psi,v) - L(u,v)}{\tau} \\ &= 2\lim_{\tau\to 0}\frac{a(u+\tau\psi,u) - a(u,u)}{\tau} + \lim_{\tau\to 0}\frac{a(u+\tau\psi,v) - a(u,v)}{\tau} \\ &= 2a(\psi,u) + a(\psi,v) \\ &= a(\psi,2u+v) \\ &\Rightarrow v = -2u \end{aligned} \tag{28}$$

Now we can get the shape derivative of the compliance $J(\Omega,u)$ as follows:

$$\begin{aligned} J_\Omega(\Omega,u) = L_\Omega &= \frac{\partial a(u,u)}{\partial\Omega} + \frac{\partial W(u,-2u)}{\partial\Omega} \\ &= \frac{\partial a(u,u)}{\partial\Omega} + \frac{\partial a(u,-2u)}{\partial\Omega} + 2\frac{\partial l(u)}{\partial\Omega}. \end{aligned} \tag{29}$$

Considering

$$\frac{\partial a(u,v)}{\partial\Omega} = \frac{1}{2}\int_\Gamma E_{ijkl}\varepsilon_{ij}(u)\varepsilon(v)V_n ds, \tag{30}$$

we get

$$\frac{\partial a(u,u)}{\partial\Omega} = \frac{1}{2}\int_\Gamma E_{ijkl}\varepsilon_{ij}(u)\varepsilon_{kl}(u)V_n ds, \tag{31}$$

$$\frac{\partial a(u,-2u)}{\partial\Omega} = -\int_\Gamma E_{ijkl}\varepsilon_{ij}(u)\varepsilon_{kl}(u)V_n ds. \tag{32}$$

At the same time, we get the shape derivative of $l(u)$, using the result in classical shape optimization [68], that is,

$$\frac{\partial l(u)}{\partial\Omega} = \int_{\Gamma_{N_1}}\left[\frac{\partial(g\cdot u)}{\partial n} + \kappa g\cdot u\right]V_n ds + \int_\Gamma f\cdot uV_n ds \tag{33}$$

Substituting the results in equations (31), (32) and (33) into

equation (29), we get the final form of $J_\Omega(\Omega,u,\omega_i)$ as follows

$$J_\Omega(\Omega,u)=2\left\{\int_{\Gamma_{N_1}}\left[\frac{\partial(g\cdot u)}{\partial n}+\kappa g\cdot u\right]V_n ds+\int_\Gamma f\cdot uV_n ds\right\}. \quad (34)$$
$$-\frac{1}{2}\int_\Gamma E_{ijkl}\varepsilon_{ij}(u)\varepsilon_{kl}(u)V_n ds$$

Since the body force f is not considered and the length of Neumann boundary is in fact zero (the force is applied at a point), in practical implementations only the last term in equation (34) is considered. Substituting equation (34) into equation (21), we get the shape gradient of the objective functional, which is denoted as follows:

$$J^*_\Omega(\Omega,u,\omega)=\mu_\Omega(J(\Omega,u,\omega))+c\sigma_\Omega(J(\Omega,u,\omega)).$$

5. RSTO ALGORITHM AND DEMONSTRATION EXAMPLES

5.1 Numerical Algorithm

The algorithm for RSTO is shown in Figure 4. After setting the initial design and boundary conditions, the spectral methods introduced in Section 2 are first introduced to reduce the dimensionality for representing the uncertainties in loading and material. For the reduced set of random variables, the locations and weights of nodes are determined next based on the Gauss-type quadrature for calculating the mean and variance of the performance function. The shape sensitivity is then calculated at each integration node. Therefore, the computational cost is proportional to the number of nodes. The velocity field is set using the steepest descent method and the geometry is updated via Hamilton-Jacobi equation. This loop will iterate until the convergence criterion is satisfied.

5.2 Demonstration Examples

The proposed robust design procedure is first applied to an example with two non-normal random variables to verify the effectiveness and feasibility of the moment calculation based on the Gauss-type quadrature formula and the proposed design sensitivity analysis. After that, we apply the proposed method to design a 3D bridge beam with consideration of a random loading field in example 2 and a random material field in example 3.

Example 1. A 2D Bridge Beam with a Random Load at Bottom

The boundary condition of the bridge beam is shown in Figure 5. The design domain is defined within a 2-by-1 square with the lower left corner fixed and the lower right corner simply supported. A random external force is applied in the middle of the top. The angle of the random force takes a uniform distribution with the interval from $-\pi$ to 0 , and the magnitude takes a Gumbel distribution with the mean equal to 1 and variance equal to 0.3. The design domain is discretized using 100-by-50 elements for elastic analysis. The elastic material is assumed with a dummy Young's modulus of $E=1$ and the Poisson ratio of 0.3. The void area is assumed with a dummy Young's modulus of 0.001 and the same Poisson ratio of 0.3. The settings in the deterministic optimization are the same as the robust optimization example, except that the force is a deterministic unit force in the vertical direction.

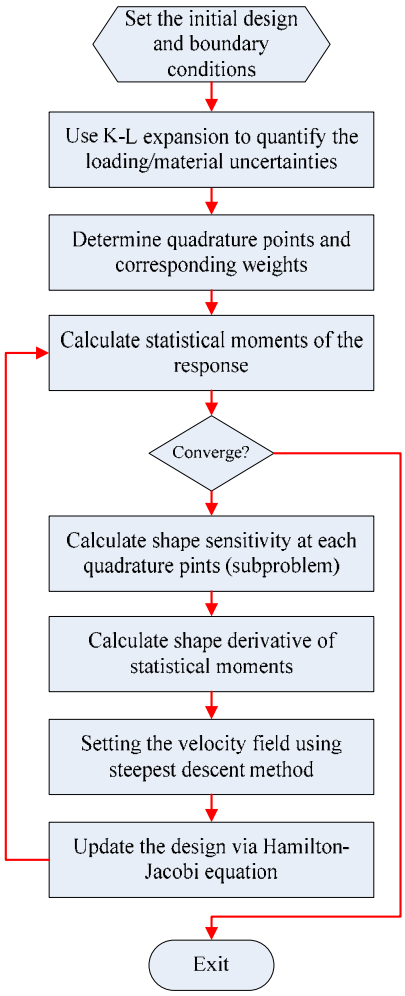

FIGURE 4: FLOWCHART OF THE RSTO ALGORITHM

In this example, a 25-point tensor product Gauss-type quadrature is used to calculate the mean and variance of the compliance at each design solution. By reducing the computational cost using the linear superposition theory, we are able to apply the Monte Carlo method with 10000 experiments to provide a standard reference. As shown in Figure 5, the topology of the robust topology design is different from that of the deterministic design. The performance and robustness of the robust and deterministic designs are compared in Table 1.

TABLE 1. COMPARISON BETWEEN ROBUST AND DETERMINISTIC DESIGNS

		Robust	Deterministic
E(C)	25-point tensor-product quadrature	25.1155	36.8167
	Monte Caro (10000 points)	25.0632	37.0326
Std(C)	25-point tensor-product quadrature	17.4334	27.5360
	Monte Caro (10000 points)	17.5861	27.1967

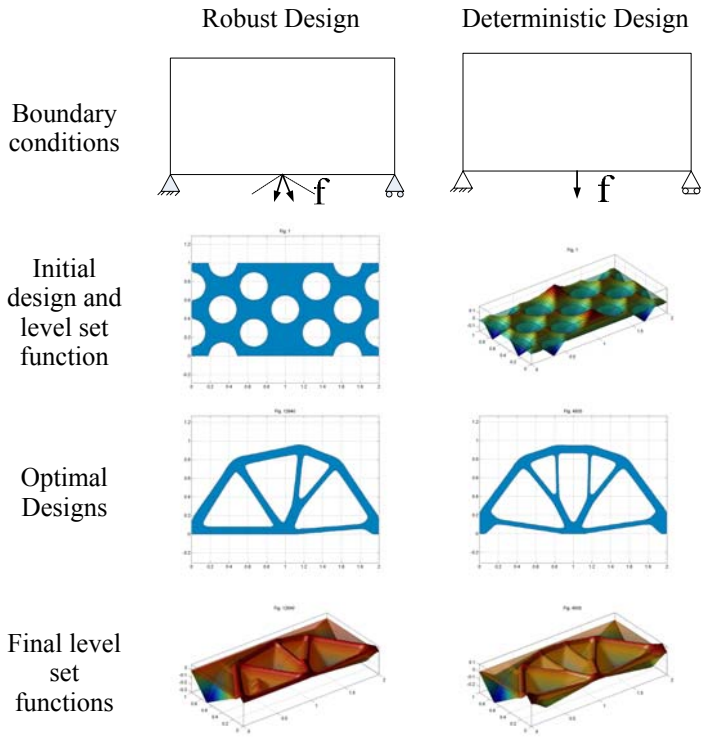

FIGURE 5: ROBUST (LEFT COLUMN) V.S. DETERMINISTIC (RIGHT COLUMN) TOPOLOGY OPTIMIZATION OF A BEAM STRUCTURE

Both the mean (25.0632) and variance (17.5861) of the robust topology design is much smaller (better) than that of the deterministic design (37.0326 and 27.1967 respectively), which means the robust topology design possesses a better performance and robustness to the deterministic design under the specified random loading condition. While most of the robust design problems involve the tradeoff between optimizing the mean performance and minimizing the performance variance, deterministic topology optimization problems only optimize the performance in a specific scenario (e.g, for a specific load magnitude and direction). Because both the magnitude and direction of a load change, it is generally not true that the mean performance of the robust design solution must be worse than that from deterministic optimization. At the same time, it is noted from Table 1 that the results of 25-point tensor product Gauss-type quadrature are very close to those of the Monte Carlo method, with much improved efficiency.

Example 2. A 3D Bridge Beam with a Random Loading Field at the Top

In this example, we optimize a 3D bridge beam considering a random loading field on the top. The boundary conditions and initial designs are shown in Figure 6 (a) and (b). The dimensions of the design domain are 2-by-0.5-by-1 (X-by-Y-by-Z). The random loading field is assumed to take a normal distribution with mean equal to 1 and standard deviation equal to 0.2. The correlation length of the random load field is set to be 0.5. In the optimization process, the level set function is evolved on a 101-by-26-by-51 Euler grid, where the design domain is discretized using about 4000 finite elements for elastic analysis. Three eigenvectors are used in uncertainty quantification and three quadrature nodes are used in the direction of each eigenvector. UDR is employed to calculate the stochastic moments, which reduces the finite element evaluation numbers from 27 to 7 in each optimization iteration.

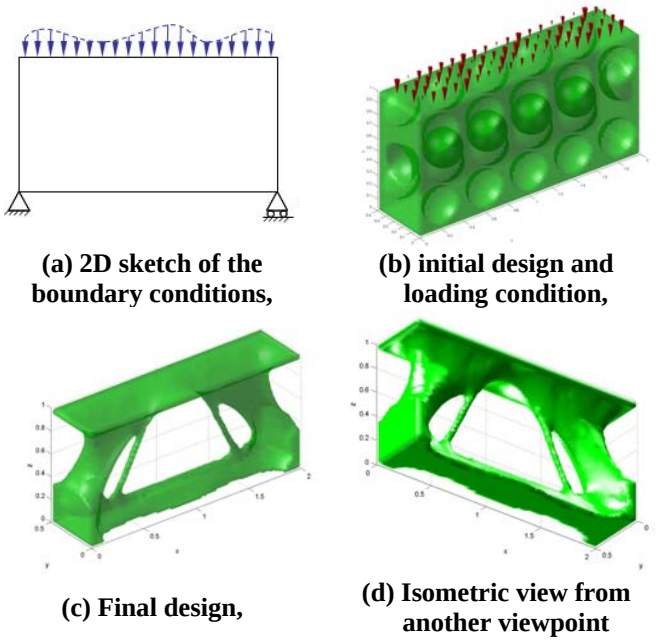

(a) 2D sketch of the boundary conditions, **(b) initial design and loading condition,**

(c) Final design, **(d) Isometric view from another viewpoint**

FIGURE 6: RSTO OF A 3D BRIDGE BEAM.

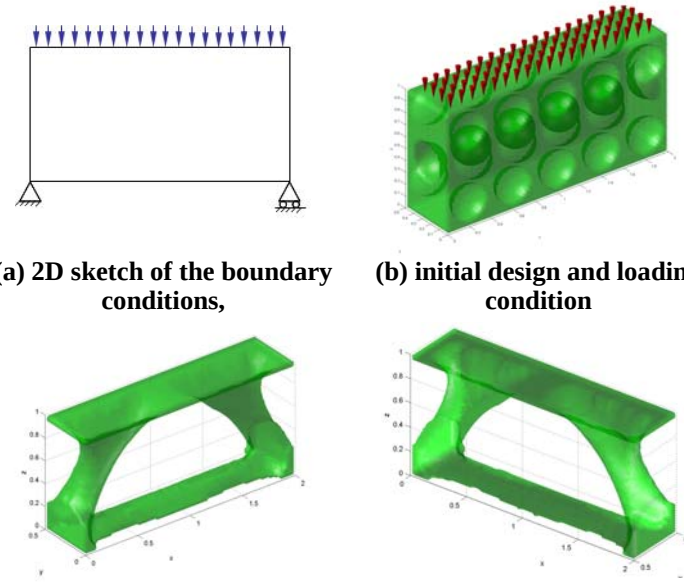

(a) 2D sketch of the boundary conditions, **(b) initial design and loading condition**

(c) Final design **(d) Isometric view from another viewpoint**

FIGURE 7: DETERMINISTIC TOPOLOGY OPTIMIZATION OF A 3D BRIDGE BEAM.

The finial design of RSTO is shown in Figure 6 (c) and (d). The corresponding deterministic result (DTO) is shown in Figure 7. Compared with the deterministic design, the robust design possesses two more ribs and a thickened beam at bottom, which can provide additional strength to the bridge under loading variations. A comparison of the mean and variance of the robust and deterministic designs are listed in Table 2. Again, the performance of a RSTO result is more robust than its deterministic counterpart, when subject to a random loading field.

TABLE 2. COMPARISON BETWEEN ROBUST AND DETERMINISTIC DESIGNS UNDER RANDOM LOADING FIELDS

	Robust	Deterministic
E(C)	19.84	22.49
Std(C)	4.64	5.24

Example 3. A 3D Bridge Beam with a Random Material Field

In this problem, a 3D bridge beam is optimized subject to a spatially-varying material property field across the design domain. The boundary condition of the problem is similar to that of example 1 and the dimensions of the design domain are the same as the setting of example 2. The material property field (Young's Modulus) is assumed to take a normal distribution with mean equal to 1 and standard deviation 0.2. A realization of the random field is shown in Figure 8 (b). An exponential function is employed to describe the correlation between any two spatial points in the random field as follows:

$$C = \exp\left(-\frac{\|X_1 - X_2\|}{d}\right). \tag{35}$$

Here $\|X_1 - X_2\|$ is the Euclidean distance between the two points and d is the correlation length which is set to be 0.5 in this example. In the optimization process, the level set function is evolved on a 101-by-26-by-51 Euler grid, and the design domain is discretized using about 4000 finite elements for elastic analysis. Due to the strong correlation, three eigenvectors are used in uncertainty quantification and the random material field can be quantified as follows:

$$g(x,\omega) = \bar{g}(x) + \sum_{i=1}^{3} \sqrt{\lambda_i}\, g_i(x)\, \xi_i(\omega). \tag{36}$$

Three quadrature nodes are used in each eigenvector direction for demonstration. The final design of RSTO is shown in Figure 8 (c) and (d). The corresponding DTO results shown in Figure 8 (e) and (f), where the Young's Modulus is a constant 1.

TABLE 3. PERFORMANCES OF ROBUST AND DETERMINISTIC DESIGNS UNDER DIFFERENT MATERIAL FIELDS

	Parameters of Material Field	Robust	Deterministic
Material Field 1	E=1	23.05	22.73
Material Field 2	$\mu_E = 1$, $\sigma_E = 0.3$, $d = 0.5$	23.25	23.48

We apply two different material fields to both the robust and the deterministic designs. The performances of robust and deterministic designs under different material fields are listed in Table 3. Results in Table 3 show that both the performance of robust design is more stable than that of deterministic design. Compared with the deterministic design, the robust design possesses obviously thicker bars while the number of bars is less than that of its deterministic counterpart, making the appearance more robust. The increased thickness of the bars makes the robust design less sensitive to the variations in the material field.

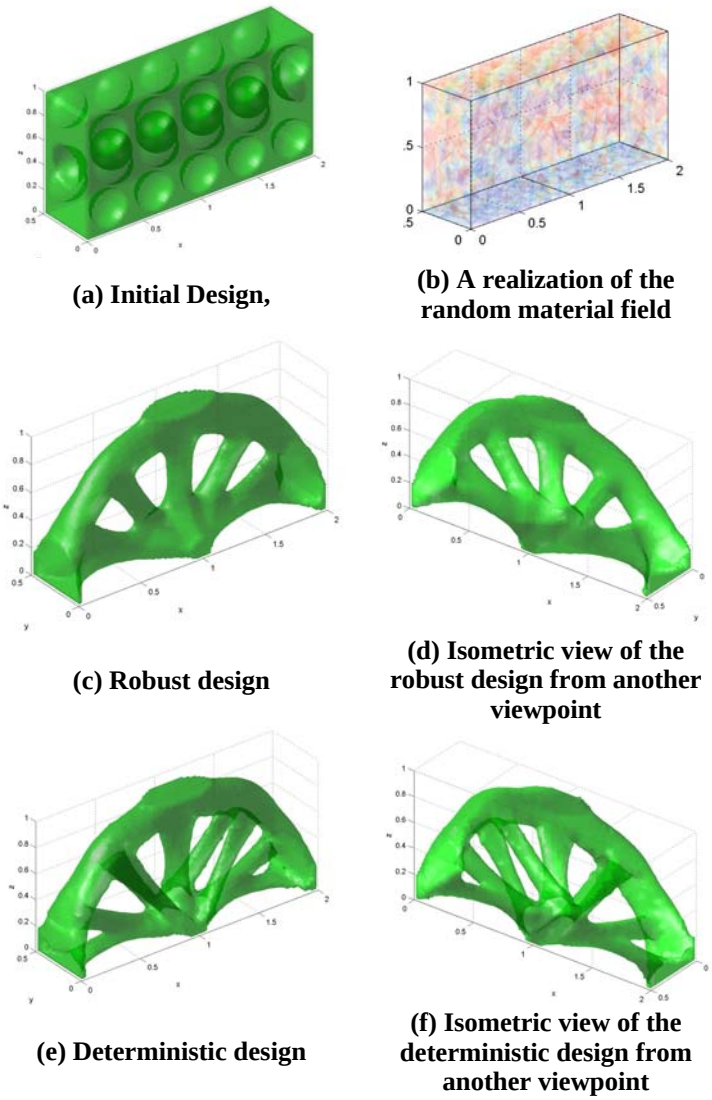

(a) Initial Design, **(b) A realization of the random material field**

(c) Robust design **(d) Isometric view of the robust design from another viewpoint**

(e) Deterministic design **(f) Isometric view of the deterministic design from another viewpoint**

FIGURE 8: ROBUST (a-d) vs. DETERMINISTIC (e-f) OPTIZATION OF A 3D BRIDGE BEAM UNDER A RANDOM MATERIAL FIELD.

6. CONCLUSIONS AND FUTURE WORK

For the first time, robust design is integrated with level set methods to implement robust shape and topology optimization. The method presented in this paper is expected to provide a mathematically rigorous and computationally viable approach to RSTO problems. The Karhunen-Loeve expansion is employed to characterize random-filed uncertainty, which is essentially a spectral representation of the random field using a reduced set of random variables and the eigenfunctions of its covariance function as expansion bases. Once the reduced set of random variables is identified, either the tensor product quadrature rule or the univariate dimension-reduction (UDR) quadrature rule is then employed for calculating statistical moments of the design response. The combination of the above techniques not only provides a computationally viable approach in evaluating the statistical moments, which otherwise would be computationally

formidable, but also enables a semi-analytical approach that introduces the shape sensitivity of the statistical moments using the adjoint variable method and calculus of variation. The shape derivative is seamlessly integrated with a level-set-based topology optimization framework via the steepest descent method. The proposed RSTO method is illustrated with bench mark examples subject to lumped random loads and a random loading/material field. The benchmark examples show that the results from RSTO may be quite different from that of the deterministic topology optimization and the RSTO designs are more robust than deterministic designs under uncertainty. Throughout our research, we also had the following observation that uncertainty is not the only factor that has impact on the topology of the final design; the interaction between the boundary condition and the uncertainties determines the topology of the final design to a large extent (keeping other conditions fixed). These issues still needs further investigations in our future research.

ACKNOWLEDGEMENT

The grant support (CMMI – 0522662) from National Science Foundation (NSF) and the support from the Center for Advanced Vehicular Systems at Mississippi State University via Department of Energy Contract No: DE-AC05-00OR22725 are greatly acknowledged.

REFERENCES

1. Bendsøe, M.P. and N. Kikuchi, *Generating optimal topologies in structural design using a homogenization method*. Computer Methods in Applied Mechanics and Engineering, 1988. **71**: p. 197-224.
2. Bendsøe, M., A. Ben-Tal, and J. Zowe, *Optimization methods for truss geometry and topology design*. Structural and Multidisciplinary Optimization, 1994: p. 141-159.
3. Rozvany, G.I.N., M. Zhou, and T. Birker, *Generalized shape optimization without homogenization*. Strutural Optimization, 1992. **4**: p. 250-254.
4. Sigmund, O., *On the Design of Compliant Mechanisms Using Topology Optimization*. Mechanics Based Design of Structures and Machines, 1997. **25**(4): p. 493-524.
5. Sigmund, O., *A 99 line topology optimization code written in MATLAB*. Structural and Multidisciplinary Optimization, 2001. **21**(2): p. 120-127.
6. Allaire, G., F. Jouve, and A.-M. Toader, *Structural optimization using sensitivity analysis and a level-set method*. Journal of Computational Physics, 2004. **194**(1): p. 363-393
7. Allaire, G., F. Jouve, and A.-M. Toader, *A level-set method for shape optimization*. C. R. Acad. Sci. Paris, Serie I, 2002. **334**: p. 1-6.
8. Wang, M.Y., X. Wang, and D. Guo, *A level set method for structural topology optimization* Computer Methods in Applied Mechanics and Engineering, 2003. **192**(1-2): p. 227-246
9. Wang, M.Y. and X.M. Wang, *PDE-driven level sets, shape sensitivity, and curvature flow for structural topology optimization*. Computer Modeling in Engineering & Sciences, 2004. **6**: p. 373-395.
10. Christiansen, S., M. Patriksson, and L. Wynter, *Stochastic bilevel programming in structural optimization* Structural and Multidisciplinary Optimization, 2001. **21**(5): p. 361-371.
11. Mogami, K., et al., *Reliability-based structural optimization of frame structures for multiple failure criteria using topology optimization techniques* Structural and Multidisciplinary Optimization, 2006. **32**(4): p. 299-311.
12. Seepersad, C.C., et al., *Robust Design of Cellular Materials With Topological and Dimensional Imperfections*. ASME Journal of Mechanical Design 2006. **128**: p. 1285-1297.
13. Kharmanda, G. and N. Olhoff, *Reliability-Based Topology Optimization as a New Strategy to Generate Different Structural Topologies*, in *15th Nordic Seminar on Computational Mechanics*. 2002: Aalborg, Denmark.
14. Jung, H.-S., S. Cho, and Y.-S. Yang, *Reliability-based Robust Topology Design Optimization of Nonlinear Structures*, in *5th World Congress of Structural and Multidisciplinary Optimization*. 2003: Lido di Jesolo, Italy.
15. Maute, K. and D.M. Frangopol, *Reliability-based design of MEMS mechanisms by topology optimization*. Computers and Structures 2003. **81** p. 813-824.
16. Jung, H.-S. and S. Cho, *Reliability-based topology optimization of geometrically nonlinear structures with loading and material uncertainties*. Finite Elements in Analysis and Design, 2004. **41** (3): p. 311-331.
17. Kharmanda, G., et al., *Reliability-based topology optimization*. Structural and Multidisciplinary Optimization, 2004. **26**(5): p. 1615-1488
18. Allen, M. and K. Maute, *Reliability-based shape optimization of structures undergoing fluid–structure interaction phenomena* Computer Methods in Applied Mechanics and Engineering 2005. **194**(30-33): p. 3472-3495
19. Chen, S.K. and M.Y. Wang, *Geometric width control in topology optimization using level set method and a quadratic energy functional*, in *of ASME 2006 International Design Engineering Technical Conferences & Computers and Information in Engineering Conference, 30th Annual Mechanisms and obotics Conference*. 2006: Philadelphia, USA.
20. Mozumder, C., et al., *An Investigation of Reliability-Based Topology Optimization Techniques*, in *Proceedings of the 11th AIAA/ISSMO Multidisciplinary Analysis and Optimization Conference,* . 2006, AIAA: Portsmouth,VA.
21. Kogiso, N., et al., *Robust Topology Optimization for Compliant Mechanisms Considering Uncertainty of Applied Loads*. Journal of Advanced Mechanical Design, Systems, and Manufacturing, 2008. **2**(1): p. 96 - 107.
22. Conti, S., et al., *Shape Optimization under Uncertainty - A Stochastic Programming Perspective*. 2008.
23. Beyer, H.-G. and B. Sendhoff, *Robust optimization - A comprehensive survey*. Computer Methods in Applied Mechanics and Engineering, 2007. **196**(33-34): p. 3190-3218.

24. Birge, J. and F. Louveaux, *Introduction to Stochastic Programming*. 1997, New York: Springer-VerLag.
25. Chen, W., et al., *A Procedure for Robust Design: Minimizing Variations Caused by Noise Factors and Control Factors*. ASME Journal of Mechanical Design, 1996. **18**(4): p. 478-485.
26. Ghanem, R.G. and P.D. Spanos, *Stochastic Finite Element Analysis, A Spectral Approach*. 1991, New York: Springer-Verlag.
27. Taguchi, G., *Taguchi on Robust Technology Development: Bringing Quality Engineering Upstream*. 1993, New York: ASME Press.
28. Phadke, M.S., *Quality Engineering using Robust Design*. 1989, Englewood Cliffs, New Jersey: Prentice Hall.
29. Nair, V.N., *Taguchi's Parameter Design: A Panel Discussion*. Technometrics, 1992. **34**: p. 128-161.
30. Wu, C.F.J. and M. Hamada, *Experiments: Planning, Analysis, and Parameter Design Optimization*. 2000, New York, NY.: John Wiley & Sons.
31. Parkinson, A., C. Sorensen, and N. Pourhassan, *A General Approach for Robust Optimal Design*. ASME Journal of Mechanical Design, 1993. **115**(1): p. 74-80.
32. Sundaresan, S., K. Ishii, and D.R. Houser, *A Robust Optimization Procedure with Variations on Design Variables and Constraints*. Advances in Design Automation , ASME DE, 1993. **69**(1): p. 379-386.
33. Su, J. and J.E. Renaud, *Automatic Differentiation in Robust Optimization*. AIAA Journal, 1997. **35**(6): p. 1072.
34. Iyer, H.V. and S. Krishnamurty, *A Preference-Based Robust Design Metric*, in *Proceedings of the 1998 ASME Design Technical Conference*. 1998: Atlanta, GA.
35. Parkinson, D.B., *The Application of a Robust Design Method to Tolerancing*. Journal of Mechanical Design, 2000. **122**(2): p. 149-154.
36. Kalsi, M., K. Hacker, and K. Lewis, *A Comprehensive Robust Design Approach for Decision Trade-Offs in Complex Systems Design*. Journal of Mechanical Design, 2001. **123**(1): p. 1-10.
37. Hernandez, G., et al., *Robust Design of Families of Products With Production Modeling and Evaluation*. Journal of Mechanical Design, 2001. **123** (2): p. 183-190.
38. Suri, R. and O. K., *Manufacturing System Robustness Through Integrated Modeling*. Journal of Mechanical Design, 2001. **123** (4): p. 630-636.
39. McAllister, C.D. and T.W. Simpson, *Multidisciplinary Robust Design Optimization of an Internal Combustion Engine*. Journal of Mechanical Design, 2003. **125** (1): p. 124-130.
40. Jin, R., X. Du, and W. Chen, *The Use of Metamodeling Techniques for Optimization under Uncertainty*. Journal of Structural & Multidisciplinary Optimization, 2003. **25**(2): p. 99-116.
41. Melchers, R.E., *Structural Reliability Analysis and Prediction*. 1999, Chichester, England: John Wiley & Sons.
42. Du, X. and W. Chen, *Towards a better understanding of modeling feasibility robustness in engineering design*. ASME Journal of Mechanical Design, 2000. **122**: p. 385-394.
43. Du, X. and W. Chen, *A Most Probable Point Based Method for Uncertainty Analysis*. Journal of Design and Manufacturing Automation, 2001. **4**: p. 47-66.
44. Tu, J. and K.K. Choi, *A New Study on Reliability Based Design Optimization*. ASME Journal of Mechanical Design, 1999. **121**(4): p. 557-564.
45. Osher, S. and J. Sethian, *Fronts propagating with curvature-dependent speed: algorithms based on hamilton-jacobi formulations*. Journal of Computational Physics, 1988. **79**: p. 12-49.
46. Sethian, J.A., *Level Set Methods and Fast Marching Methods*. 2nd ed. 1999: Cambridge University Press.
47. Osher, S. and R. Fedkiw, *Level Sets Methods and Dynamic Implicit Surfaces*. 2003: Springer.
48. Wang, M., X.M. Wang, and D.M. Guo, *A level set method for structural topology optimization*. Computer Methods in Applied Mechanics and Engineering, 2003. **192**: p. 227-246.
49. Sethian, J. and A. Wiengmann, *Structural boundary design via level set and immersed interface methods*. Journal of Computational Physics, 2000. **163**: p. 489-528.
50. Osher, S.J. and F. Santosa, *Level set methods for optimization problems involving geometry and constraints. I. frequencies of a two-density inhomogeneous drum*. Journal of Computational Physics, 2001. **171**: p. 272-288.
51. Allaire, G., F. Jouve, and A.M. Toader, *Structural optimization using sensitivity analysis and a level-set method*. Journal of Computational Physics, 2004. **194**: p. 363-393.
52. Wang, M.Y. and X.M. Wang, *'Color' level sets: A multi-phase level set method for structural topology optimization with multiple materials*. Computer Methods in Applied Mechanics and Engineering, 2004. **193**: p. 469-496.
53. Wang, M.Y., et al., *Design of multi-material compliant mechanisms using level set methods* ASME Journal of Mechanical Design, 2005. **127**(5): p. 941-956.
54. Chen, S.K. and M.Y. Wang, *Designing Distributed Compliant Mechanisms with Characteristic Stiffness*, in *of the ASME 2007 International Design Engineering Technical Conferences & Computers and Information in Engineering Conference IDETC/CIE 2007*. 2007: Las Vegas, Nevada, USA.
55. Chen, S.K., M.Y. Wang, and A.Q. Liu, *Shape feature control in structural topology optimization*. Computer-Aided Design, 2008. **40**(9): p. 951-962.
56. Reddy, J., *Applied functional analysis and variational methods in engineering*. 1986: McGraw-Hill Book Company.
57. Zabaras, N. *Spectral Methods for Uncertainty Quantification*. 2007 [cited; Available from: http://mpdc.mae.cornell.edu/.
58. Yin, X., et al., *Efficient Random Field Uncertainty Propagation in Design using Multiscale Analysis*. Journal of Mechanical Design, 2008: p. accepted.
59. Yin, X., et al. *A Multiscale Design Approach with Random Field Representation of Material Uncertainty*.

in *Proceedings of ASME 2008 International Design Engineering Technical Conferences & Computers and Information in Engineering Conference*. 2008. New York City, NY.
60. Ghanem, R.G. and P.D. Spanos, *Stochastic Finite Elements A Spectral Approach* Revised Edition ed. 1991, New York: Springer-Verlag.
61. Ghanem, R.G. and A. Doostan, *On the Construction and Analysis of Stochastic Models: Characterization and Propagation of the Errors Associated with Limited Data*. Journal of Computational Physics, 2006. **217**: p. 63-81.
62. Haldar, A. and S. Mahadevan, *Reliability Assessment using Stochastic Finite Element Analysis*. 2000, New York: John Wiley & Sons, INC.
63. Engels, H., *Numerical Quadrature and Cubature*. 1980, London: Academic Press.
64. Rahman, S. and H. Xu, *A Univariate Dimension-Reduction Method for Multi-Dimensional Integration in Stochastic Mechanics*. Probabilistic Engineering Mechanics, 2004. **19**: p. 393-408.
65. Xu, H. and S. Rahman, *A generalized dimension-reduction method for multi-dimensional integration in stochastic mechanics*. Int J Numer Methods Eng, 2004. **61**: p. 1992-2019.
66. Zhao, Y.-G. and T. Ono, *Moment Methods for Structural Reliability*. Journal of Structural Safety, 2001. **23**: p. 47-75.
67. Lee, S.H., W. Chen, and B.M. Kwak, *Robust Design with Arbitrary Distributions Using Gauss-type Quadrature Formula*. Structural and Multidisciplinary Optimization, accepted, 2008.
68. Sokolowski, J. and J.P. Zolesio, *Introduction to Shape Optimization: Shape Sensitivity Analysis*. 1992: Springer.
69. Pironneau, O., *Optimal Shape Design for Elliptic Systems*. Series in Computational Physics. 1984, New York: Springer.
70. Ta'asan, S., *Introduction to shape design and control*. 1997.